

## Rheological analysis of natural and diluted mud suspensions

Shakeel, Ahmad; Kirichek, Alex ; Chassagne, Claire

**DOI**

[10.1016/j.jnnfm.2020.104434](https://doi.org/10.1016/j.jnnfm.2020.104434)

**Publication date**

2020

**Document Version**

Final published version

**Published in**

Journal of Non-Newtonian Fluid Mechanics

**Citation (APA)**

Shakeel, A., Kirichek, A., & Chassagne, C. (2020). Rheological analysis of natural and diluted mud suspensions. *Journal of Non-Newtonian Fluid Mechanics*, 286, [104434].  
<https://doi.org/10.1016/j.jnnfm.2020.104434>

**Important note**

To cite this publication, please use the final published version (if applicable).  
Please check the document version above.

**Copyright**

Other than for strictly personal use, it is not permitted to download, forward or distribute the text or part of it, without the consent of the author(s) and/or copyright holder(s), unless the work is under an open content license such as Creative Commons.

**Takedown policy**

Please contact us and provide details if you believe this document breaches copyrights.  
We will remove access to the work immediately and investigate your claim.



## Rheological analysis of natural and diluted mud suspensions

Ahmad Shakeel<sup>a,b,\*</sup>, Alex Kirichek<sup>c</sup>, Claire Chassagne<sup>a</sup>

<sup>a</sup> Faculty of Civil Engineering and Geosciences, Department of Hydraulic Engineering, Delft University of Technology, Stevinweg 1, 2628 CN, Delft, the Netherlands

<sup>b</sup> Department of Chemical, Polymer & Composite Materials Engineering, University of Engineering & Technology, Lahore, KSK Campus, 54890, Pakistan

<sup>c</sup> Deltares, Boussinesqweg 1, 2629 HV, Delft, the Netherlands

### ARTICLE INFO

#### Keywords:

Natural mud  
Diluted mud  
Structural recovery  
Yield stress  
Moduli  
Mud density

### ABSTRACT

Natural mud usually exhibits non-Newtonian rheological behaviors like viscoelasticity, thixotropy and yield stress. The history of each mud sample is also an important factor influencing the rheological behavior, as the state of the clay fabric – for a same composition – is dependent on the shear stresses experienced previously by the sample. Several rheological tests including stress ramp-up, oscillatory frequency sweep and structural recovery tests were performed, in order to analyse the rheological fingerprint of the mud samples collected from two different locations of the Port of Hamburg. The yield stress, storage moduli and structural recovery of mud from the same location was studied as a function of density for two series of samples. One series consisted of samples (“natural samples”) taken in-situ as a function of depth (with increasing density as a function of depth) whereas the other one (“diluted samples”) consisted of samples whereby the density was varied by adding in-situ water to the natural sample having the highest density. Significant differences in rheological characteristics were found between the natural and diluted mud samples, that were attributed to the state/composition of the mud’s fabric in each situation but also to the structural rearrangements caused by the preparation of diluted samples.

### 1. Introduction

Mud consists of clay minerals, water, organic matter, silt and sand. Usually, natural mud exhibits viscoelasticity, shear-thinning, thixotropy and yield stress properties. It is already known that the rheological fingerprint of mud samples is dependent on their density and that the presence of small amounts of organic matter can significantly affect their rheological behavior [1, 2].

Steady and oscillatory rheological measurements are rheological methods for studying natural mud [3–10]. Van Kessel and Bloom analysed the rheological properties of estuarine mud and kaolinite clay samples. They investigated the viscoelastic behavior of their samples in oscillatory mode at small strains [6]. Soltanpour and Samsami performed the comparative rheology of kaolinite clay and Hendijan mud from northwest part of Persian Gulf using frequency sweep and flow curve tests [11]. Their results revealed a strong dependence of the rheological parameters on the water content of the samples. Xu and Huhe reported the rheological analysis of estuarine mud at Lianyungang, China with the help of both steady and dynamic rheological methods [12]. They found an exponential increase in the yield stress of their mud samples as a function of increasing volume fraction of solids.

Fonseca et al. [13] studied the steady rheological properties of mud sediments from Port of Santos, the Port of Itajaí, the Port of Rio Grande and the Amazon south navigation channel in Brazil. An exponential relation between the yield stress and the density of mud samples was observed. Aubry et al. [14] investigated the rheological properties of natural estuarine mud samples. The material properties of the samples were fitted using an exponential function of the density.

Recently, Shakeel et al. [15] reported the rheological properties of mud sediments having different consistencies (defined as fluid mud, pre-consolidated mud and consolidated mud) collected from different locations of Port of Hamburg (Germany) using steady and oscillatory rheological methods. These different mud layers can exist in the ports and waterways and correspond to different stages of mud consolidation. All these layers can have significantly different thicknesses and rheological characteristics, with increasing density as a function of depth. We refer to “natural samples” as the samples of different densities taken in-situ as a function of depth. In literature, the rheological behavior as a function of mud density is typically investigated by step-by-step dilution of a high density mud. We refer to these type of samples as “diluted samples” in this study. The aim of the present article is to study whether natural and diluted mud samples exhibit a comparable yield

\* Corresponding author.

E-mail addresses: [A.Shakeel@tudelft.nl](mailto:A.Shakeel@tudelft.nl) (A. Shakeel), [Alex.Kirichek@deltares.nl](mailto:Alex.Kirichek@deltares.nl) (A. Kirichek), [C.Chassagne@tudelft.nl](mailto:C.Chassagne@tudelft.nl) (C. Chassagne).

<https://doi.org/10.1016/j.jnnfm.2020.104434>

Received 30 May 2020; Received in revised form 20 October 2020; Accepted 21 October 2020

Available online 31 October 2020

0377-0257/© 2020 The Author(s). Published by Elsevier B.V. This is an open access article under the CC BY license (<http://creativecommons.org/licenses/by/4.0/>).

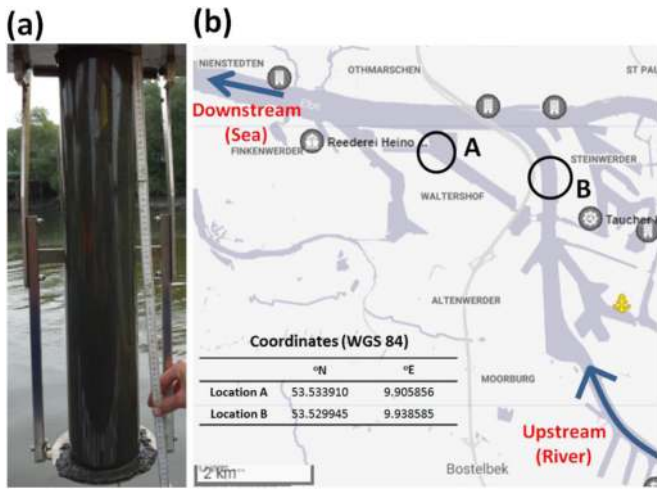


Fig. 1. (a) Frahmnot core sampler (b) selected locations in the Port of Hamburg, Germany for collecting mud samples.

stress/density dependence. The differences observed between natural and diluted mud samples in terms of yield stress, storage modulus and structural recovery after breakup are presented along with the discussion on the origin of these differences.

2. Experimental

In this study, mud samples were collected from two different locations (A and B) of the Port of Hamburg, Germany using one meter core sampler (Fig. 1a and b). The collected core samples were subsampled into different layers based on the differences in their consolidation stage. The samples were packed in the sealed containers and transported to the laboratory. The dry density of the sediments was assumed to be 2650 kg/m<sup>3</sup> [3] and the bulk density was obtained by using the method reported elsewhere [3]. This bulk density was in good agreement with the bulk density measured using an Anton Paar portable density meter (DMA 35). Particle size distributions within the different mud layers were measured using static light scattering (Malvern MasterSizer 2000MU). The mud samples were extensively diluted with water, in order to have the laser obstruction of the device within the required range. The results are presented in Fig. 2a and b. The characteristics of the natural mud layers along with their sample ID are summarized in Table 1. Samples A6 and B4 were diluted with the water from the same locations and gently mixed by hand, in order to test the mud samples having same composition but different density. The densities of these diluted samples are presented in Table 2. Before conducting rheological

experiments, all the mud samples were homogenized by mild hand stirring.

Rheological experiments were performed using a HAAKE MARS I rheometer (Thermo Scientific, Germany) with concentric cylinder geometry (gap width = 1 mm). A waiting time of 3–5 min was used before the experiment to eliminate the disturbances created by the bob after attaining its measurement position. The temperature was maintained at 20 °C during each experiment using a Peltier controller system. Each

Table 1 Characteristics of the natural mud layers from locations A and B.

Sample ID	Density (kg/m <sup>3</sup> )	D <sub>10</sub> (μm)	D <sub>50</sub> (μm)	D <sub>90</sub> (μm)
<b>Samples from Location A</b>				
A0	1.03 × 10 <sup>3</sup>	4.8	14.8	59
A1	1.11 × 10 <sup>3</sup>	5.0	14.7	56
A2	1.12 × 10 <sup>3</sup>	4.3	14.5	64
A3	1.13 × 10 <sup>3</sup>	4.3	14.8	65
A4	1.15 × 10 <sup>3</sup>	4.4	15.3	73
A5	1.29 × 10 <sup>3</sup>	4.9	18.4	86
A6	1.33 × 10 <sup>3</sup>	4.7	18.6	92
<b>Samples from Location B</b>				
B0	1.04 × 10 <sup>3</sup>	5.1	15.9	64
B1	1.09 × 10 <sup>3</sup>	4.7	16.1	68
B2	1.11 × 10 <sup>3</sup>	4.5	16.3	82
B3	1.11 × 10 <sup>3</sup>	4.6	15.9	70
B4	1.16 × 10 <sup>3</sup>	4.4	16.1	92

Table 2 Characteristics of the diluted mud layers obtained from samples A6 and B4.

Sample ID	Density (kg/m <sup>3</sup> )
<b>Diluted Samples from Sample A6</b>	
A6D1	1.10 × 10 <sup>3</sup>
A6D2	1.14 × 10 <sup>3</sup>
A6D3	1.17 × 10 <sup>3</sup>
A6D4	1.18 × 10 <sup>3</sup>
A6D5	1.20 × 10 <sup>3</sup>
A6D6	1.22 × 10 <sup>3</sup>
A6D7	1.23 × 10 <sup>3</sup>
A6D8	1.25 × 10 <sup>3</sup>
A6D9	1.27 × 10 <sup>3</sup>
A6D10	1.28 × 10 <sup>3</sup>
A6D11	1.30 × 10 <sup>3</sup>
<b>Diluted Samples from Sample B4</b>	
B4D1	1.07 × 10 <sup>3</sup>
B4D2	1.12 × 10 <sup>3</sup>
B4D3	1.13 × 10 <sup>3</sup>
B4D4	1.14 × 10 <sup>3</sup>
B4D5	1.15 × 10 <sup>3</sup>

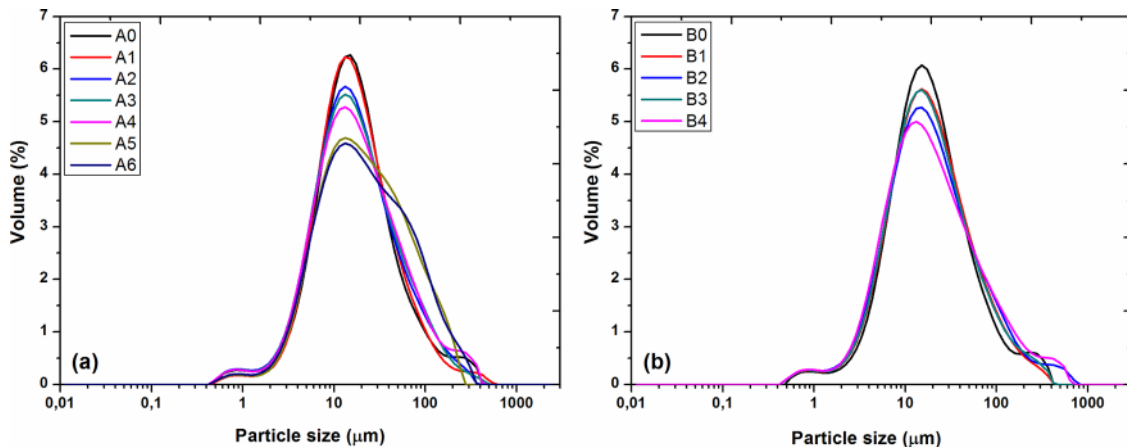


Fig. 2. Particle size distribution of natural mud layers from (a) location A and (b) location B.

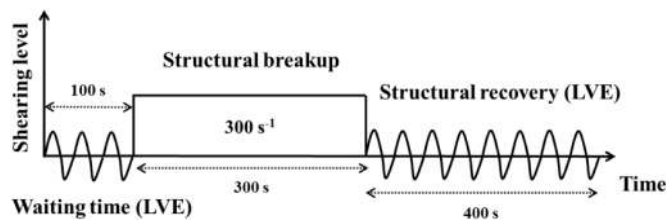


Fig. 3. Pictorial representation of the structural recovery test.

experiment was carried out in duplicate to check the repeatability of the measurements. The repeatability error was always less than 2%. Grooved Couette geometry was also used, in order to investigate wall slip phenomenon, which is very common for these kind of samples [16]. The results revealed the absence of wall slip by displaying similar results when either smooth or grooved Couette geometries were used (data not shown). The following rheological tests were performed to analyse the mud samples:

2.1. Stress ramp-up test

Stress ramp-up tests are performed using the stress controlled mode of the rheometer. An increasing stress is applied at a rate of 0.1–10 Pa/s, depending upon the consistency of the sample, until the shear rate reaches  $300 \text{ s}^{-1}$ . The corresponding torque is measured, and the shear rate and viscosity are then determined.

2.2. Frequency sweep test

Preliminary amplitude sweep tests are carried out at a constant fre-

quency of 1 Hz to estimate the linear viscoelastic (LVE) regimes. Frequency sweep tests are then performed from 0.1 to 100 Hz within the linear viscoelastic regime. The selected amplitude for frequency sweep tests is tuned for each sample based on the results of preliminary amplitude sweep tests. The storage modulus ( $G'$ ), and loss modulus ( $G''$ ) are recorded as a function of frequency.

2.3. Structural recovery test

Structural recovery test is performed by adopting a three step protocol reported elsewhere [17]. In short, the protocol starts with a waiting time of 100 s (i.e., oscillatory time sweep within LVE regime at 1 Hz) after the bob has reached its measurement position. This time is sufficient to eliminate the disturbances created by the insertion of the bob. Moreover it also enables to estimate the storage modulus before the structural breakup. A steady shearing step is then performed at a shear rate of  $300 \text{ s}^{-1}$  for 300 s. After that, a structural recovery step is carried out by performing oscillatory time sweep experiments within the linear viscoelastic regime at a frequency of 1 Hz for 400 s (Fig. 3). Preliminary amplitude sweep tests are also performed to determine the LVE region for both oscillatory steps of the protocol.

3. Results and discussion

3.1. Yield stress measurements

In order to analyse the effect of dilution on the yield stress of mud sediments, stress ramp-up tests were performed at a rate of 0.1–1 Pa/s to determine the yield stress values of natural and diluted mud layers. Fig. 4a–d show the outcome of these stress ramp-up tests, for natural and diluted mud layers from locations A and B, in the form of apparent

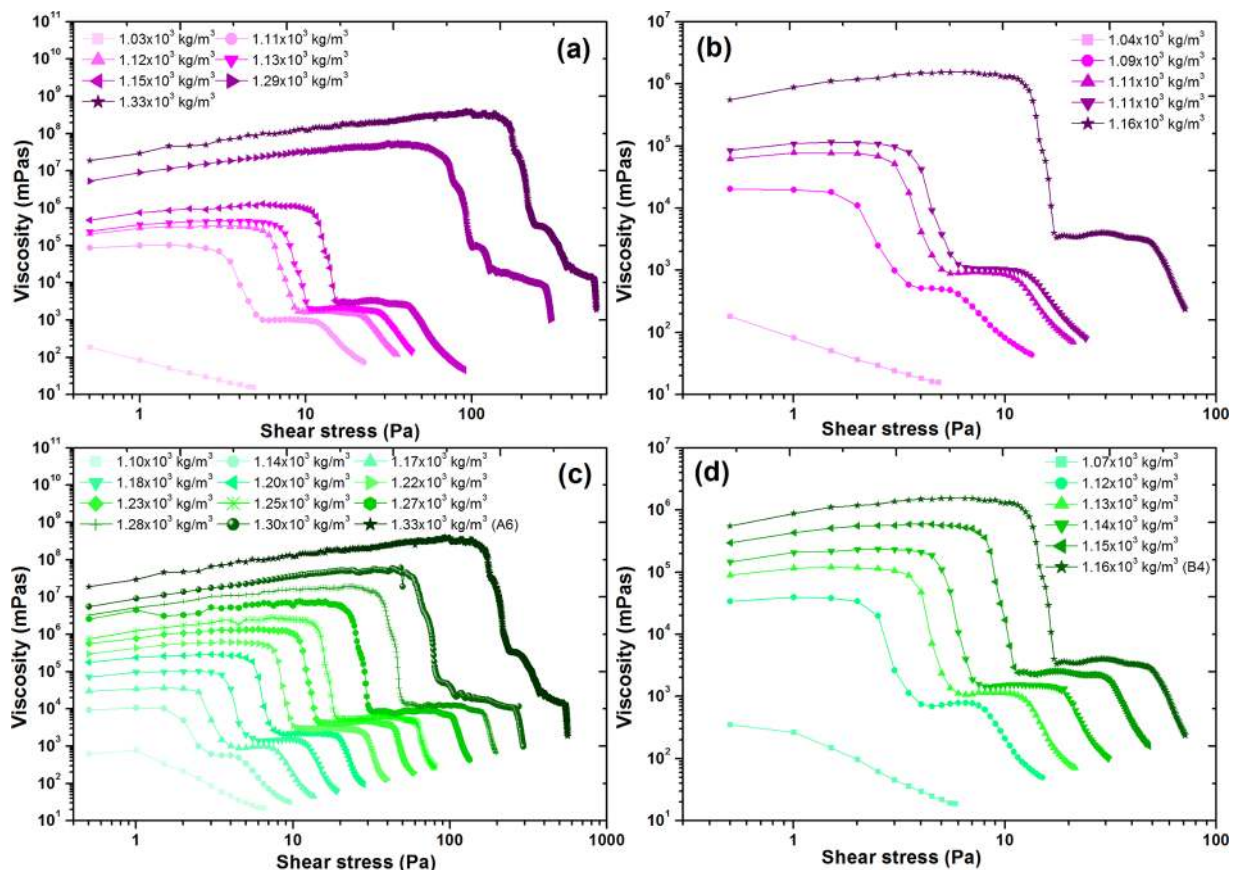


Fig. 4. Apparent viscosity as a function of shear stress for natural mud layers from (a) location A and (b) location B and diluted mud layers from (c) location A and (d) location B.



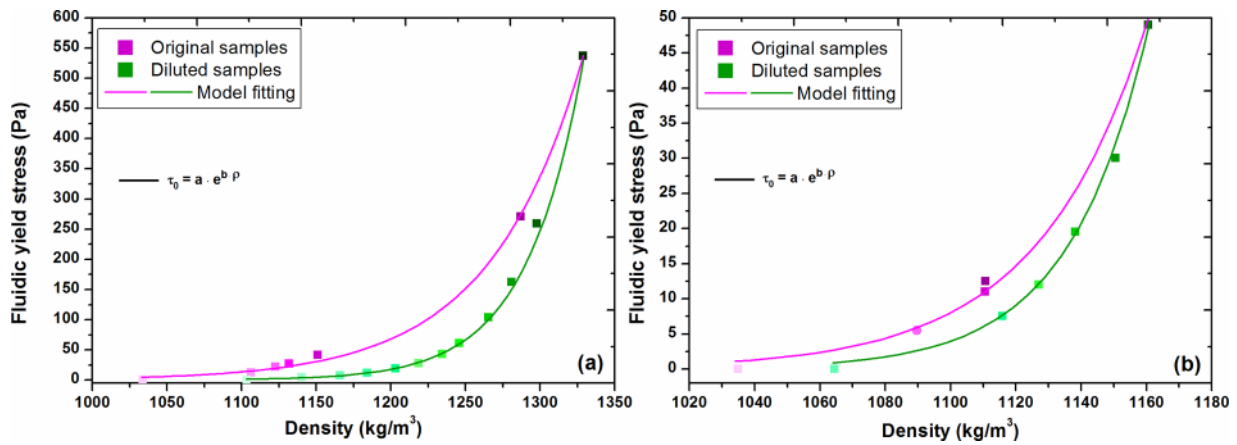


Fig. 5. Fluidic yield stress values as a function of bulk density for natural (original) and diluted mud layers from (a) location A and (b) location B. Solid lines represent the model fitting.

**Table 3**  
Values of the model parameters for natural and diluted mud layers.

Location	Mud Layers	a (Pa)	Std Error	b (m <sup>3</sup> /kg)	Std Error	R <sup>2</sup>
A	Original	$3.6 \times 10^{-7}$	$2.1 \times 10^{-7}$	0.016	0.0004	0.99
	Diluted	$5.5 \times 10^{-12}$	$3.9 \times 10^{-12}$	0.024	0.0005	0.99
B	Original	$4.7 \times 10^{-13}$	$7.7 \times 10^{-13}$	0.028	0.0014	0.99
	Diluted	$4.3 \times 10^{-16}$	$2.1 \times 10^{-15}$	0.034	0.0042	0.99

viscosity as a function of shear stress. From these stress-viscosity curves, the two yield stress values were determined from the two sharp declines in viscosity (i.e., two-step yielding) [18]. The first decline is referred to as static yield stress,  $\tau_y^s$ , while the second one is termed as fluidic yield

stress,  $\tau_y^f$  [15]. These two declines may be attributed to the existence of two levels of structure in the mud samples. The analogous two-step yielding behavior was also observed for different systems including colloidal gel [19], colloidal glasses [20], magneto-rheological systems [21], carbopol microgel [22], muscovite dispersions [23], natural mud suspensions [15], etc. Furthermore, the transition from two-step yielding to one-step yielding or no-yielding was also evident at lower densities due to the liquid-like nature of the samples. A similar transition from two-step yielding to single-step yielding, as a function of volume fraction of solids, has also been reported in literature for magneto-rheological suspensions [24].

The fluidic yield stress values of natural (original) and diluted mud

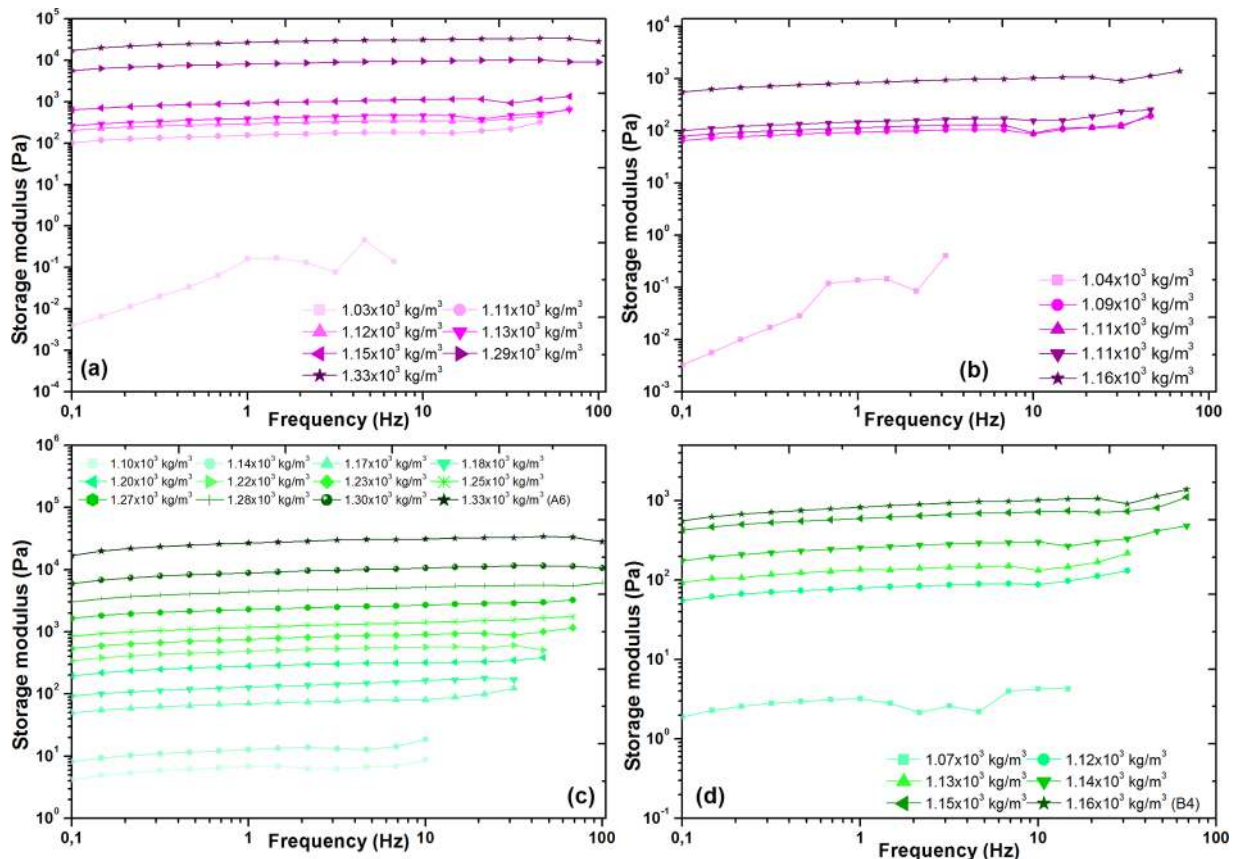


Fig. 6. Storage modulus as a function of frequency for natural mud layers from (a) location A and (b) location B and diluted mud layers from (c) location A and (d) location B.

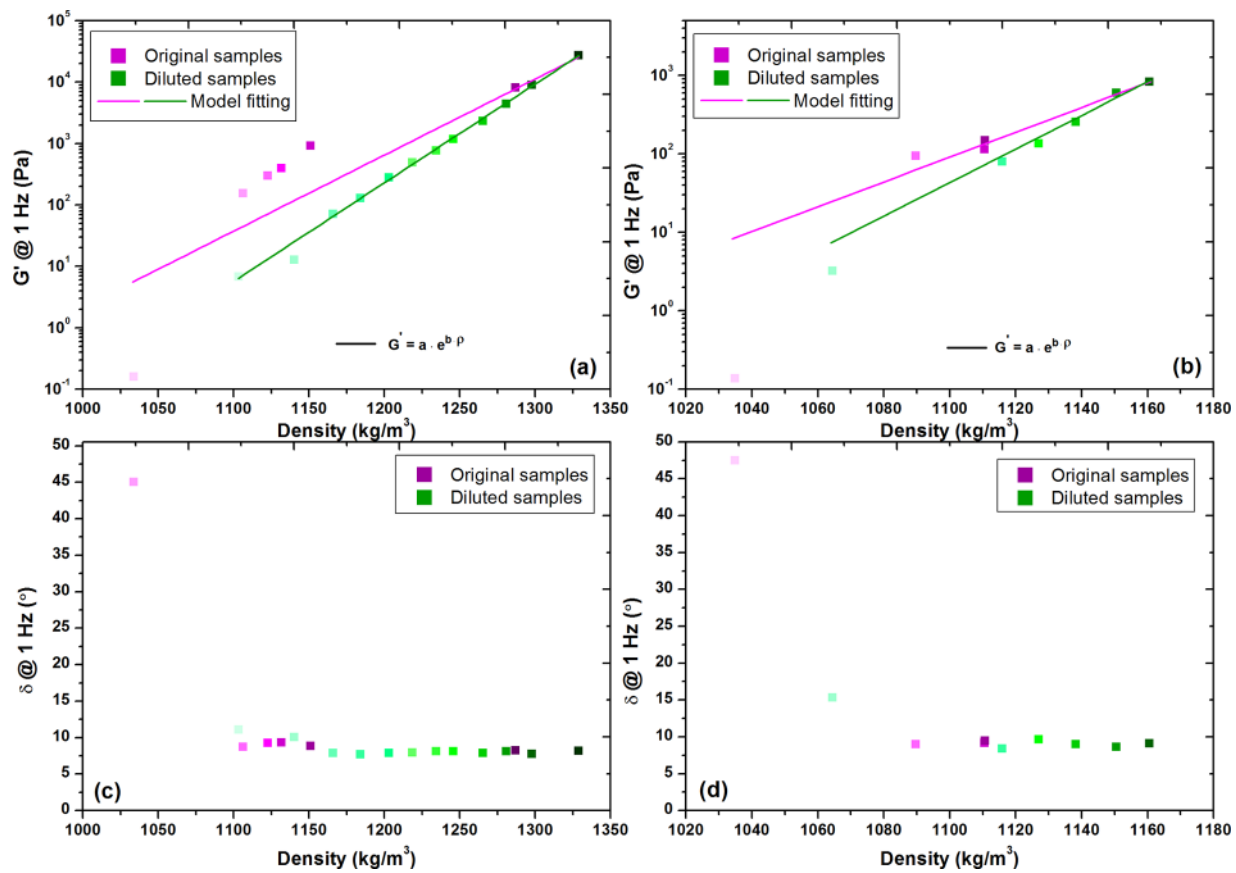


Fig. 7. Storage modulus ( $G'$ ) values at 1 Hz as a function of bulk density for natural (original) and diluted mud layers from (a) location A and (b) location B. Solid lines represent the model fitting. Phase angle ( $\delta$ ) values at 1 Hz as a function of bulk density for natural (original) and diluted mud layers from (c) location A and (d) location B.

**Table 4**  
Values of the model parameters for natural and diluted mud layers.

Location	Mud Layers	a (Pa)	Std Error	b ( $m^3/kg$ )	Std Error	R <sup>2</sup>
A	Original	$9.1 \times 10^{-13}$	$1.4 \times 10^{-12}$	0.029	0.0012	0.99
	Diluted	$2.1 \times 10^{-15}$	$3.7 \times 10^{-15}$	0.033	0.0012	0.99
B	Original	$2.1 \times 10^{-14}$	$5.8 \times 10^{-14}$	0.033	0.0024	0.99
	Diluted	$3.6 \times 10^{-17}$	$2.8 \times 10^{-16}$	0.038	0.0066	0.98

layers as a function of density for locations A and B are presented in Fig. 5a and b, respectively. Both natural and diluted mud layers displayed an exponential increase in yield stress as a function of density, for both locations. A similar exponential increase in yield stresses as a function of density has been reported in literature for different mud sediments [8, 10, 25]. However, it is clearly evident that, for both locations, the dependency of yield stress on density is significantly different for diluted mud as compared to natural mud samples. For all density values, diluted mud samples showed lower yield stress values as compared to natural mud samples. The same results were obtained for the static yield stress values (data not shown). The experimental data of yield stress values as a function of density was fitted with an empirical exponential relation. The difference in yield stress behavior as a function of density for natural and diluted mud samples is also evident when comparing the different values of the model parameters (Table 3).

### 3.2. Storage modulus measurements

Apart from yield stress measurements, frequency sweep tests were also performed within linear viscoelastic regime to determine the storage moduli of natural and diluted mud layers. Preliminary amplitude

sweep tests were performed to find the linear viscoelastic regime for all the samples. Fig. 6a–d show the results of frequency sweep tests in the form of storage modulus as a function of frequency for natural and diluted mud layers obtained from locations A and B. This test is typically conducted for studying the mechanical properties of the system without disturbing the structure of the material. It can be easily seen that the storage modulus of all the mud samples, except the ones with lower densities, was more or less frequency independent, which confirms the solid-like behavior of the samples over the complete range of studied frequencies. The analogous solid-like behavior (frequency independent modulus) of the mud sediments as a function of frequency within LVE regime was also described in the literature [6, 11, 12]. At higher frequencies, an increase in storage modulus was observed, which was not attributed to the system behavior but rather to the inertial problems within the instrumentation at such high frequencies (data removed from the graphs). The mud samples with lower densities displayed a significant frequency dependency of storage modulus. In this case, the inertial problems were very prominent, even at frequencies as low as 2 Hz, triggered by the liquid-like nature of these samples.

The storage modulus at 1 Hz was plotted as a function of density for natural (original) and diluted mud layers from locations A and B (Fig. 7a and b). An exponential increase in the storage modulus as a function of density is found for both natural and diluted mud layers. A similar increase in storage modulus of mud sediments as a function of volume fraction was also reported by Huang and Aode [8]. However, it is also clearly evident that the relationship between storage modulus and density is different for diluted and natural mud samples. For all density values, lower storage modulus values were found for diluted mud as compared to natural mud. An empirical exponential relation was used in both cases to fit the experimental data of storage modulus as a function

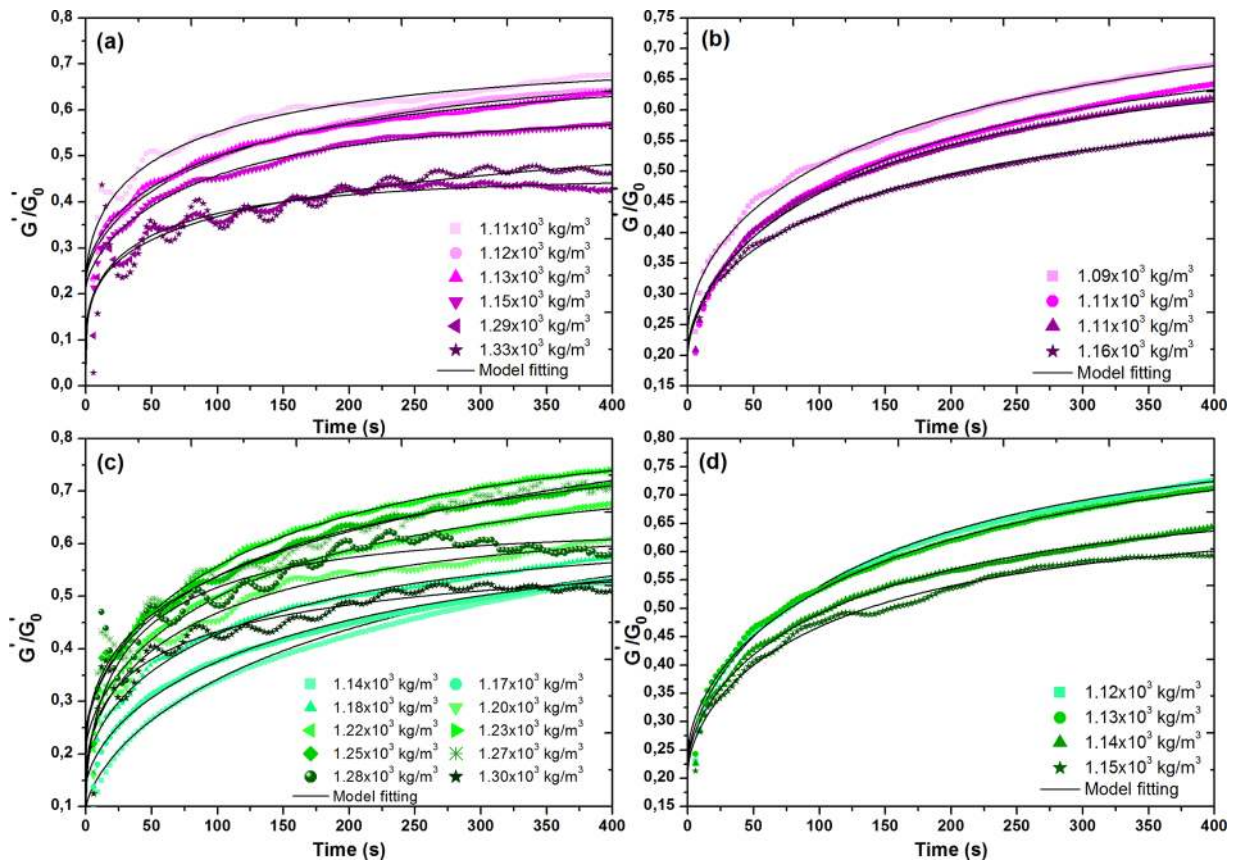


**Fig. 8.** Normalized storage modulus as a function of recovery time for natural mud layers from (a) location A and (b) location B and diluted mud layers from (c) location A and (d) location B.

of density. The difference in storage modulus behavior as a function of density for natural and diluted mud samples is also evident when comparing the values of the model parameters (Table 4). Furthermore, the mud samples (natural or diluted) displayed a solid-like behavior as evident from smaller phase angle values (Fig. 7c and d). The samples having lowest densities even showed a cross-over in frequency sweep test (i.e.,  $\delta = 45^\circ$ ) and hence exhibited liquid-like behavior, as already depicted by yield stress analysis.

### 3.3. Structural recovery measurements

The structural recovery after shearing in natural and diluted mud

samples was analysed by the structural recovery protocol described in Section 2.3. A waiting step was performed for each sample to measure the initial structure level ( $G'_0$ ) of the samples before shearing. The structural growth in terms of normalized storage modulus (i.e., with respect to initial storage modulus) as a function of time is shown in Fig. 8a–d for natural and diluted mud samples obtained from locations A and B. The oscillations observed in the recovery response, particularly for higher density samples, may be attributed to the elasticity of the samples [17, 26]. It is found that the structural recovery,  $G'/G'_0$  in natural mud samples decreases with increasing density, for both locations. A similar behavior was observed in the case of diluted mud samples from location B (Fig. 8d) while the diluted samples from location A displayed

**Table 5**  
Values of the model parameters for natural and diluted mud layers from location A.

Sample ID	$G'_\infty$ (Pa)	Std Error	$t_r$ (s)	Std Error	$d$ (-)	Std Error	$R^2$ (-)	$G'_\infty/G'_0$
<b>Samples from Location A</b>								
A1	$1.13 \times 10^2$	2.3	80	9	0.52	0.03	0.96	0.72
A2	$2.02 \times 10^2$	2.1	135	6	0.65	0.01	0.99	0.66
A3	$2.80 \times 10^2$	3.5	121	7	0.62	0.02	0.99	0.63
A4	$5.03 \times 10^2$	3.5	94	3	0.71	0.02	0.99	0.59
A5	$3.83 \times 10^3$	63.9	51	4	0.56	0.04	0.92	0.46
A6	$1.6 \times 10^4$	7177	47	4	0.41	0.07	0.80	0.44
<b>Diluted Samples of A6</b>								
A6D2	$2.20 \times 10^1$	0.5	248	17	0.68	0.01	0.99	0.69
A6D3	$5.00 \times 10^1$	0.9	185	12	0.65	0.01	0.99	0.63
A6D4	$8.9 \times 10^1$	1.1	121	6	0.66	0.02	0.99	0.61
A6D5	$1.74 \times 10^2$	3.2	96	8	0.60	0.02	0.98	0.64
A6D6	$3.26 \times 10^2$	4.1	145	7	0.66	0.01	0.99	0.74
A6D7	$6.04 \times 10^2$	7.1	151	7	0.66	0.01	0.99	0.81
A6D8	$9.9 \times 10^2$	23.9	164	17	0.58	0.02	0.99	0.82
A6D9	$2.53 \times 10^3$	55.8	195	15	0.38	0.04	0.96	0.81
A6D10	$2.77 \times 10^3$	63.9	81	6	0.54	0.05	0.85	0.63
A6D11	$4.8 \times 10^3$	232.4	43	9	0.45	0.04	0.90	0.59

**Table 6**  
Values of the model parameters for natural and diluted mud layers from location B.

Sample ID	$G'_{\infty}$ (Pa)	Std Error	$t_r$ (s)	Std Error	$d$ (-)	Std Error	$R^2$ (-)	$G'_{\infty}/G'_0$
<b>Samples from Location B</b>								
B1	$3.70 \times 10^1$	0.7	184	16	0.60	0.01	0.99	0.75
B2	$8.1 \times 10^1$	1.1	162	9	0.66	0.01	0.99	0.72
B3	$9.7 \times 10^1$	1.2	149	8	0.66	0.01	0.99	0.72
B4	$6.4 \times 10^2$	13.0	137	10	0.60	0.02	0.99	0.67
<b>Diluted Samples of B4</b>								
B4D2	$6.20 \times 10^1$	0.6	149	6	0.68	0.01	0.99	0.81
B4D3	$1.17 \times 10^2$	1.9	141	7	0.63	0.01	0.99	0.74
B4D4	$1.96 \times 10^2$	2.2	136	7	0.64	0.01	0.99	0.70
B4D5	$3.56 \times 10^2$	5.3	129	9	0.64	0.02	0.99	0.66

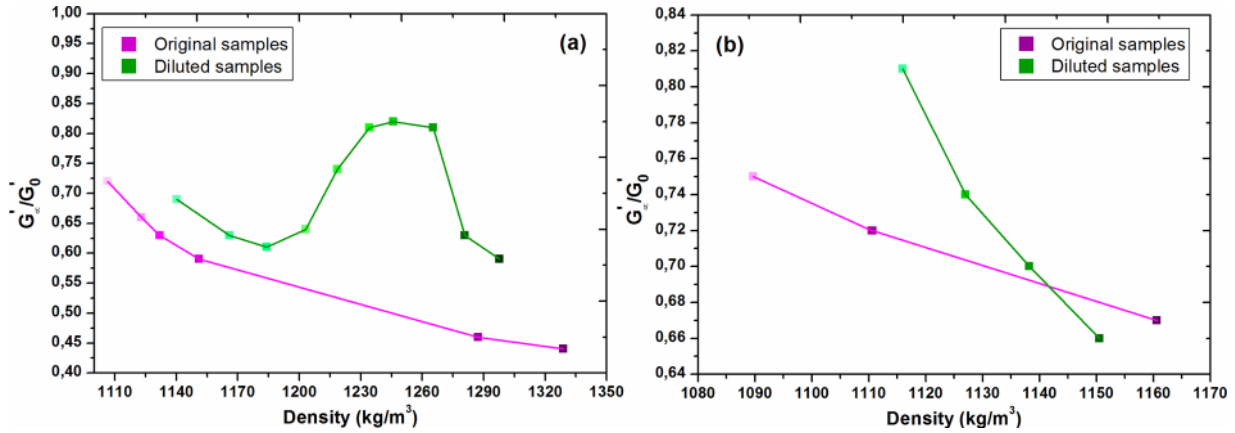


**Fig. 9.** Normalized extent of structural recovery as a function of density for natural (original) and diluted mud layers from (a) location A and (b) location B. Solid lines are just the guide for the eye.

completely different behavior (Fig. 8c).

A simple model adapted from [27] was used to fit the data of storage modulus as a function of time after pre-shearing, given as follows:

$$\frac{G'}{G'_0} = \frac{G'_i}{G'_0} + \left( \left( \frac{G'_{\infty} - G'_i}{G'_0} \right) \left( 1 - \exp \left[ - \left( \frac{t}{t_r} \right)^d \right] \right) \right) \quad (1)$$

where  $G'$  is the time dependent storage modulus of samples after shearing,  $G'_0$  is the storage modulus before structural breakup,  $G'_i$  is the storage modulus right after pre-shearing and  $G'_{\infty}$  is the storage modulus at  $t \rightarrow \infty$ ;  $t_r$  is the characteristic time of the material;  $d$  is a stretching exponent and its value lies within the range of 0–1. The fitting parameters in the Eq. (1) are  $G'_{\infty}$ ,  $t_r$  and  $d$ . The values of these fitting parameters are presented in Tables 5 and 6 for mud samples from location A and location B, respectively.

The normalized extent of structural recovery ( $G'_{\infty}/G'_0$ ) is also plotted as a function of density for natural and diluted mud samples from locations A and B (Fig. 9a and b). For location A, the natural samples displayed a decrease in structural recovery as a function of density while the diluted samples exhibited a significantly different behavior with a

maxima in the structural recovery curve. In case of location B, the overall behavior of structural recovery as a function of density for both natural and diluted mud samples was more or less similar (i.e., decreasing structural recovery with increasing density). However, the extent of structural recovery was bit higher for the diluted samples as compared to the natural samples.

### 3.4. Discussion

As already mentioned, the differences in rheological properties of mud layers can be linked to several parameters i.e., mud composition,

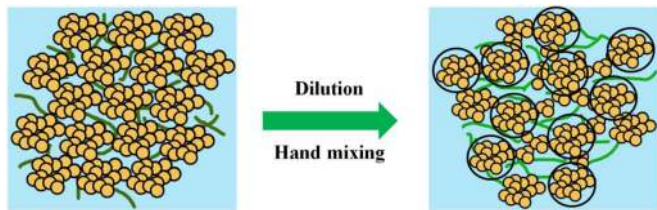


**Fig. 10.** Schematic representation of structural rearrangements in mud sample after dilution via hand mixing. Yellow circles represent clay particles, green lines represent organic matter and black circles represent the clay aggregates.

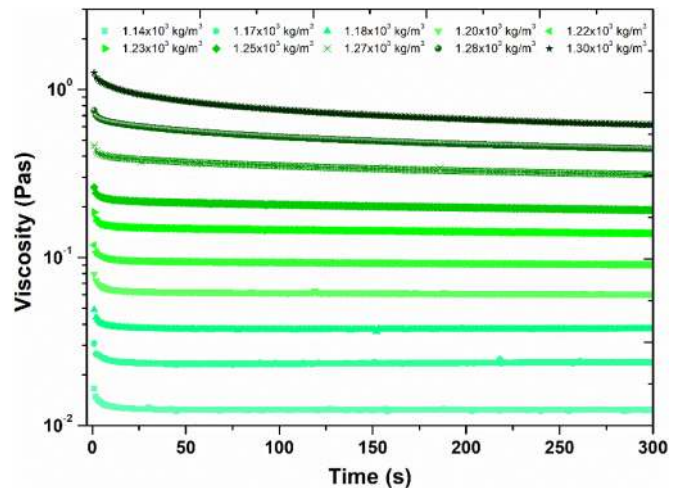


**Fig. 11.** Apparent viscosity as a function of time at a shear rate of  $300 \text{ s}^{-1}$  during pre-shear step for diluted mud samples from location A.



type and content of organic matter, ionic concentration, particle size distribution, etc. [15, 28], which explains the differences between the rheological features of natural and diluted mud samples. Furthermore, the observed differences in rheological properties (i.e., yield stress and storage modulus) as a function of density for natural and diluted mud samples may be attributed to the formation of heterogeneous microstructures by diluting the mud samples. These heterogeneous structures are likely to be created as hand mixing was used to prepare the diluted samples. This gentle mixing method was preferred to keep the mud as undisturbed as possible. Therefore, we hypothesize that by diluting a mud suspension using hand mixing, the resulting system will be composed of large aggregates which will interconnect at rest with each other to form a space filling network. The resulting interconnected network will be weaker than the original one due to the presence of wider spaces between structure, resulting in lower yield stress or moduli (Fig. 10). A similar mechanism has been proposed in literature for describing the decrease in compressive yield stress as a function of volume fraction, by diluting aggregated alumina suspensions [29].

The structural recovery behavior of diluted mud samples from location A is quite interesting (Fig. 9a). By diluting the initial dense mud sample, the extent of structural recovery ( $G_{\infty}/G_0$ ) is first observed to increase and then to decrease. It is hypothesized that the dilution of initial dense mud sample resulted in a floc network with wider spaces and larger aggregates (Fig. 10). This floc network may then break down into smaller flocs or individual particles during the pre-shear step of the structural recovery protocol. During the structural recovery step, a more homogenous and stronger aggregate network is subsequently formed, which will display a better structural recovery.

However, after a critical dilution, further dilution of the mud samples results in a network structure of smaller aggregates as it becomes easier to break the original flocs by hand mixing. The pre-shearing step for these samples is, therefore, not able to extensively disturb the structure and the resulting structural recovery is observed to decrease. This behavior is also evident from the viscosity evolution as a function of time during pre-shear step (Fig. 11). The pre-shearing step extensively disturbed the dense mud samples ( $1265\text{--}1298\text{ kg/m}^3$ ) as evident from significant decrease in viscosity even after 300 s. However, for lower density samples, a slight decrease in viscosity is observed initially but it remains more or less constant after that initial decrease, which verified the occurrence of less disturbance for these samples. A similar increase in structural recovery as a function of applied shear rate during pre-shear step was also reported in literature for mud samples [17], which was linked to the extent of structural breakdown and rearrangements. However, in case of diluted mud samples from location B, this particular feature (i.e., peak value in structural recovery) is not observed (Fig. 9b) because of the lower densities of these samples as compared to the location A. This behavior shows that the size of the aggregates, formed after dilution, is significantly dependent on both the degree of mixing and the concentration/density of the mud samples.

All these results show that the diluted mud samples have significantly different rheological properties particularly yield stresses, storage moduli and structural recovery as compared to the natural mud samples. Extensive mixing (i.e., by ultrasonic shaking, high-speed shearing, etc.) of mud samples after dilution can provide homogenous systems but the floc network and the clay fabric will then be totally different from the ones found in-situ conditions.

#### 4. Conclusions

In this article, it is shown that natural mud samples and artificially made samples ("diluted mud samples"), obtained by diluting the dense/consolidated mud samples from the same area, can exhibit considerably different rheological behavior. A detailed rheological analysis was performed on natural and diluted mud samples, whereby the mud was collected from two different locations of Port of Hamburg, Germany.

Stress ramp-up tests, oscillatory frequency sweep tests and structural recovery tests were performed to analyse the rheological properties of mud samples.

The static and fluidic yield stress values, storage moduli and structural recovery of the natural and diluted mud sediments were significantly dissimilar from each other. The yield stress and storage moduli of all mud samples displayed an exponential increase with increasing density. Despite having the same particle size distribution, natural and diluted mud samples had nonetheless a significantly different exponential dependency on density. These differences can be attributed to a difference in organic composition (and particularly the state of oxidation) between the layers as a function of depth. The very peculiar behavior of the normalized extent of structural recovery as a function of density for the diluted mud samples was attributed to the structural heterogeneity caused by the preparation of these samples by hand mixing. Further research work is required to explain the effect of the non-mineral fraction of the mud on its rheological properties.

#### Declaration of Competing Interest

The authors declare that they have no known competing financial interests or personal relationships that could have appeared to influence the work reported in this paper.

#### Acknowledgement

This study is funded by the Hamburg Port Authority and carried out within the framework of the MUDNET academic network: <https://www.tudelft.nl/mudnet/>.

#### References

- [1] A. Shakeel, A. Kirichek, C. Chassagne, Is density enough to predict the rheology of natural sediments? *Geo-Marine Lett.* 39 (2019) 427–434.
- [2] R. Wurpts, 15 years experience with fluid mud: definition of the nautical bottom with rheological parameters, *Terra et Aqua* (2005).
- [3] P. Coussot, *Mudflow Rheology and Dynamics*, CRC Press, Rotterdam, 1997.
- [4] P. Coussot, Rheophysics of pastes: a review of microscopic modelling approaches, *Soft Matter* 3 (2007) 528–540.
- [5] F. Jiang, A.J. Mehta, Mudbanks of the Southwest Coast of India IV: mud viscoelastic properties, *J. Coast. Res.* 11 (1995) 918–926.
- [6] T. Van Kessel, C. Blom, Rheology of cohesive sediments: comparison between a natural and an artificial mud, *J. Hydraul. Res.* 36 (1998) 591–612.
- [7] B. Babatope, P.R. Williams, D.J.A. Williams, Cohesive sediment characterization by combined sedimentation and rheological measurements, *J. Hydraul. Eng.* 134 (2008) 1333–1336.
- [8] Z. Huang, H. Aode, A laboratory study of rheological properties of mudflows in Hangzhou Bay, China, *Int. J. Sediment Res.* 24 (2009) 410–424.
- [9] Y.C. Bai, C.O. Ng, H.T. Shen, S.Y. Wang, Rheological properties and incipient motion of cohesive sediment in the Haihe Estuary of China, *China Ocean Eng.* 16 (2002) 483–498.
- [10] R.W. Fass, S.I. Wartel, Rheological properties of sediment suspensions from Eckernförde and Kieler Förde Bays, Western Baltic Sea, *Int. J. Sediment Res.* 21 (2006) 24–41.
- [11] M. Soltanpour, F. Samsami, A comparative study on the rheology and wave dissipation of kaolinite and natural Hendijan Coast mud, the Persian Gulf, *Ocean Dyn.* 61 (2011) 295–309.
- [12] J. Xu, A. Huhe, Rheological study of mudflows at Lianyungang in China, *Int. J. Sediment Res.* 31 (2016) 71–78.
- [13] D.L. Fonseca, P.C. Marroig, J.C. Carneiro, M.N. Gallo, S.B. Vinzón, Assessing rheological properties of fluid mud samples through tuning fork data, *Ocean Dyn.* 69 (2019) 51–57.
- [14] T. Aubry, T. Razafinimaro, R.S. Jacinto, P. Bassoulet, Rheological properties of a natural estuarine mud, *Appl. Rheol.* 13 (2003) 142–149.
- [15] A. Shakeel, A. Kirichek, C. Chassagne, Rheological analysis of mud from Port of Hamburg, Germany, *J. Soil. Sediment.* 20 (2020) 2553–2562.
- [16] H.A. Barnes, A review of the slip (wall depletion) of polymer solutions, emulsions and particle suspensions in viscometers: its cause, character, and cure, *J. Non-newton. Fluid Mech.* 56 (1995) 221–251.
- [17] A. Shakeel, A. Kirichek, C. Chassagne, Effect of pre-shearing on the steady and dynamic rheological properties of mud sediments, *Mar. Pet. Geol.* 116 (2020), 104338.
- [18] A. Shakeel, A. Kirichek, C. Chassagne, Yield stress measurements of mud sediments using different rheological methods and geometries: an evidence of two-step yielding, *Mar. Geol.* (2020), 106247.

- [19] H.K. Chan, A. Mohraz, Two-step yielding and directional strain-induced strengthening in dilute colloidal gels, *Phys. Rev. E* 85 (2012), 041403.
- [20] K.N. Pham, G. Petekidis, D. Vlassopoulos, S.U. Egelhaaf, W.C.K. Poon, P.N. Pusey, Yielding behavior of repulsion- and attraction-dominated colloidal glasses, *J. Rheol.* 52 (2008) 649–676.
- [21] J.P. Segovia-Gutiérrez, C.L.A. Berli, J.D. Vicente, Nonlinear viscoelasticity and two-step yielding in magnetorheology: a colloidal gel approach to understand the effect of particle concentration, *J. Rheol.* 56 (2012) 1429–1448.
- [22] Z. Shao, A.S. Negi, C.O. Osuji, Role of interparticle attraction in the yielding response of microgel suspensions, *Soft Matter* 9 (2013) 5492–5500.
- [23] A. Nosrati, J. Addai-Mensah, W. Skinner, Rheology of aging aqueous muscovite clay dispersions, *Chem. Eng. Sci.* 66 (2011) 119–127.
- [24] J.C. Fernández-Toledano, J. Rodríguez-López, K. Shahrivar, R. Hidalgo-Álvarez, L. Elvira, F.M.D. Espinosa, J.D. Vicente, Two-step yielding in magnetorheology, *J. Rheol.* 58 (2014) 1507–1534.
- [25] J.S. O'Brien, P.Y. Julien, Laboratory analysis of mudflow properties, *J. Hydraul. Eng.* 114 (1988) 877–887.
- [26] T.B. Goudoulas, N. Germann, Viscoelastic properties of polyacrylamide solutions from creep ringing data, *J. Rheol.* 60 (2016) 491–502.
- [27] C. Mobuchon, P.J. Carreau, M.-C. Heuzey, Structural analysis of non-aqueous layered silicate suspensions subjected to shear flow, *J. Rheol.* 53 (2009) 1025–1048.
- [28] F. Zander, T. Heimovaara, J. Gebert, Spatial variability of organic matter degradability in tidal Elbe sediments, *J. Soil. Sediment.* (2020).
- [29] G.M. Channell, K.T. Miller, C.F. Zukoski, Effects of microstructure on the compressive yield stress, *AIChE J.* 46 (2000) 72–78.